

## Magnetically Responsive Biodegradable Nanoparticles Enhance Adenoviral Gene Transfer in Cultured Smooth Muscle and Endothelial Cells

Michael Chorny, Ilia Fishbein, Ivan Alferiev, and Robert J. Levy\*

*The Division of Cardiology, The Children's Hospital of Philadelphia,  
Philadelphia, Pennsylvania 19104*

Received January 15, 2009; Revised Manuscript Received June 4, 2009; Accepted June 4, 2009

**Abstract:** Replication-defective adenoviral (Ad) vectors have shown promise as a tool for gene delivery-based therapeutic applications. Their clinical use is however limited by therapeutically suboptimal transduction levels in cell types expressing low levels of Coxsackie-Ad receptor (CAR), the primary receptor responsible for the cell entry of the virus, and by systemic adverse reactions. Targeted delivery achievable with Ad complexed with biodegradable magnetically responsive nanoparticles (MNP) may therefore be instrumental for improving both the safety and efficiency of these vectors. Our hypothesis was that magnetically driven delivery of Ad affinity-bound to biodegradable MNP can substantially increase transgene expression in CAR deficient vascular cells in culture. Fluorescently labeled MNP were formulated from polylactide with inclusion of iron oxide and surface-modified with the D1 domain of CAR as an affinity linker. MNP cellular uptake and GFP reporter transgene expression were assayed fluorimetrically in cultured endothelial and smooth muscle cells using  $\lambda_{\text{ex}}/\lambda_{\text{em}}$  of 540 nm/575 nm and 485 nm/535 nm, respectively. Stable vector-specific association of Ad with MNP resulted in formation of MNP–Ad complexes displaying rapid cell binding kinetics following a brief exposure to a high gradient magnetic field with resultant gene transfer levels significantly increased compared to free vector or nonmagnetic control treatment. Multiple regression analysis suggested a mechanism of MNP–Ad mediated transduction distinct from that of free Ad, and confirmed the major contribution of the complexes to the gene transfer under magnetic conditions. The magnetically enhanced transduction was achieved without compromising the cell viability or growth kinetics. The enhancement of adenoviral gene delivery by affinity complexation with biodegradable MNP represents a promising approach with a potential to extend the applicability of the viral gene therapeutic strategies.

**Keywords:** Magnetic nanoparticle; adenoviral gene delivery; particle–virus hybrid system; affinity complexation; magnetically enhanced gene transfer

### Introduction

Gene therapy has the potential to radically change the treatment strategies for many human diseases or provide the only effective treatments for some that remain without cure. However, the full realization of this potential requires a

significant improvement of the existing gene delivery vectors with respect to their efficacy and/or safety. Replication-deficient adenoviruses (Ad) have been extensively investigated for gene delivery applications due to a number of advantages, including high cloning capacity (up to 37 kb) and the ability to transduce both quiescent and dividing cells without integration into the host cell genome.<sup>1</sup> Their clinical use with systemic nonlocalized delivery is however hampered

\* Address for correspondence: Robert J. Levy, M.D., The Abramson Pediatric Research Center, Suite 702, The Children's Hospital of Philadelphia, 3615 Civic Center Blvd., Philadelphia, PA 19104. Phone: 215 590 6119. Fax: 215 590 5454. E-mail: levyr@email.chop.edu.

(1) Palmer, D.; Ng, P. Improved system for helper-dependent adenoviral vector production. *Mol. Ther.* **2003**, 8, 846–52.

by adverse reactions, including thrombocytopenia,<sup>2</sup> acquired immune responses mediated by cytotoxic T lymphocytes against viral and/or transgene products,<sup>3,4</sup> and a potentially life-threatening systemic cytokine syndrome due to activation of innate immunity.<sup>5–7</sup> The latter acute toxic effects exhibit a steep dependence on the vector dose. Their occurrence varies substantially between subjects, and their likelihood cannot be readily predicted on an individual basis.<sup>6</sup> In addition to the above-mentioned untoward effects, the limited ability to confine the vector to its site of action and prevent its dissipation to nontarget tissues also contributes to compromised therapeutic efficiency. Other limitations include therapeutically suboptimal transduction levels in cell types deficient in Cocksackie-Ad receptor (CAR),<sup>8,9</sup> a cell protein involved in Ad attachment and infection.<sup>10</sup> Previously we demonstrated that delivery of Ad complexed with biodegradable nanoparticles (NP) significantly enhanced its capacity for transduction of vascular cells expressing low levels of CAR.<sup>11</sup> The increase in gene transfer efficiency was associated with a shift to a CAR-independent mechanism of Ad internalization in the form of NP–Ad affinity complexes that was not observed with control NP having no affinity for Ad. This cell uptake pathway may be kinetically favorable in the cell types where Ad–CAR interaction appears to be the

rate-limiting step of the infection process.<sup>12</sup> The present study investigated the hypothesis that the transduction efficiency of NP–Ad complexes can be further increased by using a magnetically guided delivery approach. Magnetic targeting is a promising strategy that, if successfully translated into the clinical setting, can provide a means for controlling the biodistribution of the vector, and may therefore be instrumental for improving both the safety and efficiency of the current experimental gene therapeutic methods. Magnetically responsive NP (MNP) formed with inclusion of iron oxide in the biodegradable polymeric core as reported previously<sup>13</sup> were shown to possess high specific susceptibility and negligible magnetic remanence, and enabled potent nonviral transfection of vascular cells after magnetic field exposure when formulated as ion-pair complexes with plasmid DNA.<sup>13</sup> In this study we explore the combined effect of the affinity complexation and magnetically enhanced delivery on Ad-mediated transduction by extending the utility of MNP to the formulation of magnetically responsive Ad affinity complexes (MNP–Ad). Ad binding affinity was imparted to polylactide-based MNP via modification with the recombinant immunoglobulin domain of CAR (D1) following particle surface chemical activation by a method developed in our previous study.<sup>11</sup> The gene transfer efficiency of MNP–Ad was studied in cultured vascular cells in relation to their uptake, and the transduction was compared to that observed with free Ad with or without nonimmune IgG-modified MNP, or nonmagnetic NP–Ad used as controls. The effect of magnetic vs nonmagnetic conditions and the MNP or Ad formulation amounts on gene transfer was addressed in additional experiments. Finally, the kinetics of transgene expression, MNP elimination and growth of MNP–Ad treated cells were investigated.

## Experimental Section

**Materials.** Type 5 replication-deficient Ad encoding GFP under the control of CMV promoter (GFPAd) was obtained from the Gene Vector Core Facility of the University of Pennsylvania. Poly(D,L-lactide) ( $M_r$  75,000–120,000) was obtained from Sigma-Aldrich (St. Louis, MO). Nonimmune sheep IgG (nIgG) was purchased from Cedarlane Laboratories (Hornby, ON, Canada). The human recombinant D1 domain of CAR was prepared as described elsewhere.<sup>14</sup> All chemicals were of analytical grade.

**Nanoparticle Formulation.** Magnetically responsive nanoparticles were prepared by a modification of the emulsifi-

- (2) Othman, M.; Labelle, A.; Mazzetti, I.; Elbatarny, H. S.; Lillcrap, D. Adenovirus-induced thrombocytopenia: the role of von Willebrand factor and P-selectin in mediating accelerated platelet clearance. *Blood* **2007**, *109* (7), 2832–9.
- (3) Morral, N.; O'Neal, W.; Zhou, H.; Langston, C.; Beaudet, A. Immune responses to reporter proteins and high viral dose limit duration of expression with adenoviral vectors: comparison of E2a wild type and E2a deleted vectors. *Hum. Gene Ther.* **1997**, *8* (10), 1275–86.
- (4) Tripathy, S. K.; Black, H. B.; Goldwasser, E.; Leiden, J. M. Immune responses to transgene-encoded proteins limit the stability of gene expression after injection of replication-defective adenovirus vectors. *Nat. Med.* **1996**, *2*, 545–50.
- (5) Schnell, M. A.; Zhang, Y.; Tazelaar, J.; Gao, G. P.; Yu, Q. C.; Qian, R.; Chen, S. J.; Varnavski, A. N.; LeClair, C.; Raper, S. E.; Wilson, J. M. Activation of innate immunity in nonhuman primates following intraportal administration of adenoviral vectors. *Mol. Ther.* **2001**, *3* (5 Part 1), 708–22.
- (6) Raper, S. E.; Chirmule, N.; Lee, F. S.; Wivel, N. A.; Bagg, A.; Gao, G. P.; Wilson, J. M.; Batshaw, M. L. Fatal systemic inflammatory response syndrome in a ornithine transcarbamylase deficient patient following adenoviral gene transfer. *Mol. Genet. Metab.* **2003**, *80*, 148–58.
- (7) Marshall, E. Gene therapy death prompts review of adenovirus vector. *Science* **1999**, *286*, 2244–5.
- (8) Mizuguchi, H.; Hayakawa, T. Targeted adenovirus vectors. *Hum. Gene Ther.* **2004**, *15*, 1034–44.
- (9) Parker, A. L.; Nicklin, S. A.; Baker, A. H. Interactions of adenovirus vectors with blood: implications for intravascular gene therapy applications. *Curr. Opin. Mol. Ther.* **2008**, *10*, 439–48.
- (10) Carson, S. D. Receptor for the group B coxsackieviruses and adenoviruses: CAR. *Rev. Med. Virol.* **2001**, *11*, 219–26.
- (11) Chorny, M.; Fishbein, I.; Alferiev, I. S.; Nyanguile, O.; Gaster, R.; Levy, R. J. Adenoviral gene vector tethering to nanoparticle surfaces results in receptor-independent cell entry and increased transgene expression. *Mol. Ther.* **2006**, *14*, 382–91.

- (12) Pandori, M.; Hobson, D.; Sano, T. Adenovirus-microbead conjugates possess enhanced infectivity: a new strategy for localized gene delivery. *Virology* **2002**, *299*, 204–12.
- (13) Chorny, M.; Polyak, B.; Alferiev, I. S.; Walsh, K.; Friedman, G.; Levy, R. J. Magnetically driven plasmid DNA delivery with biodegradable polymeric nanoparticles. *FASEB J.* **2007**, *21*, 2510–9.
- (14) Nyanguile, O.; Dancik, C.; Blakemore, J.; Mulgrew, K.; Kaleko, M.; Stevenson, S. C. Synthesis of adenoviral targeting molecules by intein-mediated protein ligation. *Gene Ther.* **2003**, *10*, 1362–9.

cation—solvent evaporation method, and surface-activated using a photoreactive agent, polyallylamine-benzophenone-maleimido-carboxylate (P BMC). P BMC was synthesized as previously described<sup>11</sup> by random N-acylation of polyallylamine with benzophenone, maleimido and succinamoyl residues at a molar ratio of 1:2:2, respectively. The composition of the product was confirmed by <sup>1</sup>H NMR (in DMSO-*d*<sub>6</sub>).<sup>11</sup>

An aqueous phase was prepared by dissolving 10 mg of P BMC and 6.7 mg of potassium bicarbonate in 15 mL of water. To form an organic phase, magnetite obtained from 300 mg of ferric chloride hexahydrate and 150 mg of ferrous chloride tetrahydrate reacted with an equivalent amount of sodium hydroxide was magnetically separated and coated with oleic acid (150 mg) dissolved in 4 mL of ethanol with heating to 90 °C under argon for 5 min. Excess oleic acid was phase-separated by dropwise addition of water (4 mL). The precipitate was washed with 4 mL of ethanol, dried under argon, and reconstituted in 5 mL of chloroform. The obtained organic ferrofluid was used to dissolve 200 mg of a 19:1 mixture of plain PLA and PLA covalently labeled with BODIPY<sub>564/570</sub> (Invitrogen, Eugene, OR). The magnetite incorporation step was omitted in the formulation of analogous nonmagnetic NP.

An oil-in-water emulsion was formed by sonication on ice with simultaneous pH adjustment by adding 1 mL of MES buffer, pH 5.5 (2-(*N*-morpholino)ethane sulfate, 0.1 M). Chloroform was removed using a rotary evaporator. Solid MNP were filtered through a 1.0 μm glass fiber prefilter (Millipore, Bedford, MA), exposed to long-wave UV for 5 min to achieve covalent attachment of the photoreactive P BMC to the MNP surface, and washed by 2 cycles of magnetic sedimentation—reconstitution in MES buffer, pH 6.5 (0.01 M) to remove unbound P BMC. Surface-activated MNP thus obtained were modified with the thiolated human recombinant D1 domain of CAR (or nIgG used as a control) as described elsewhere.<sup>11</sup> MNP lyophilized with 10% trehalose were kept at −20 °C and resuspended in deionized water before use.

**Cell Culture Experiments.** The effects of the relevant variables on MNP—Ad mediated gene transfer were studied in confluent and dividing vascular cells as follows. Rat aorta smooth muscle cells (A10) and bovine aorta endothelial cells (BAEC) were seeded at densities of 10<sup>4</sup>/well or 2 × 10<sup>3</sup>/well on 96-well plates for the experiments with confluent or dividing cells, respectively. In experiments addressing the effects of magnetic responsiveness and affinity complexation the transduction efficiency of Ad (1.5 × 10<sup>7</sup> viral particles/well) associated with D1-coated MNP was compared to that of Ad alone or in combination with nIgG-modified MNP, or nonmagnetic NP used as controls. All particle types were applied at doses equivalent to 1.9 μg of PLA. In a separate set of experiments examining the effects of magnetic exposure and the formulation amounts of MNP and Ad serial dilutions of GFP encoding Ad and D1-coated MNP were prepared in the dose ranges of 0 to 7.1 × 10<sup>7</sup> viral particles/well and 0 to 1.9 μg PLA/well, respectively. A series of

MNP—Ad formulations were then formed at varying concentrations of MNP and Ad covering all respective formulation amount combinations. Ad was incubated for 15 min with D1-coated MNP or control particle types and then applied to the cells in 10% FBS-supplemented DMEM for 15 min. For magnetically enhanced transduction the cell plate was placed on top of a 96-well magnetic separator with an average field gradient of 32.5 T/m as a magnetic field source (LifeSep 96F, Dexter Magnetic Technologies, Fremont, CA). The cells were then washed twice and incubated with fresh cell culture medium.

To measure the affinity complex internalization and GFP expression, the medium was replaced with phosphate buffered saline and the fluorescent signal was assayed in live cells at predetermined time points using λ<sub>ex</sub>/λ<sub>em</sub> of 540 nm/575 nm and 485 nm/535 nm, respectively. Gene transfer efficiency was expressed as the absolute GFP fluorescent signal or the ratio of the GFP signals measured in the cells treated with affinity complex formulations and free GFP-Ad. Cell viability and growth kinetics were determined using the Alamar Blue assay.<sup>15</sup> Untreated cells were used as a reference.

**Statistical Analysis.** Results were analyzed by multiple regression using the Marquardt—Levenberg algorithm<sup>16</sup> to obtain the best fit between a model equation and experimental data. ANOVA was used to validate the model and estimate the significance and relative contributions of the variables. The statistical testing was performed using SigmaStat 3.0.1 software applying iteration, step size and tolerance values of 100, 100 and 0.0001, respectively. The results were expressed as mean ± standard deviation. Differences were termed significant at *p* < 0.05.

## Results

MNP coated with an Ad binding protein, D1, were formulated with a narrow size distribution and an average diameter of 400–420 nm as determined by photon correlation spectroscopy and transmission electron microscopy (Figure 1A). The particles were near-spherical in shape and were shown to contain a large number of relatively uniform magnetite grains distributed in the polymeric matrix (Figure 1A). The high loading of magnetite configured in numerous small-sized (below 15 nm) crystallites embedded in the particle is responsible for the high magnetic susceptibility of MNP and their negligible magnetic remanence as demonstrated previously.<sup>13,17</sup> MNP affinity complexes exhibit multivalency with respect to Ad; each individual MNP particle was capable of accommodating several virions on its surface (Figure 1B) in agreement with the behavior observed with analogous nonmagnetic particles.<sup>11</sup>

- (15) O'Brien, J.; Wilson, I.; Orton, T.; Pognan, F. Investigation of the Alamar Blue (resazurin) fluorescent dye for the assessment of mammalian cell cytotoxicity. *Eur. J. Biochem.* **2000**, *267*, 5421–6.
- (16) Marquardt, D. W. An Algorithm for Least Squares Estimation of Nonlinear Parameters. *J. Soc. Ind. Appl. Math.* **1963**, *11*, 431–41.



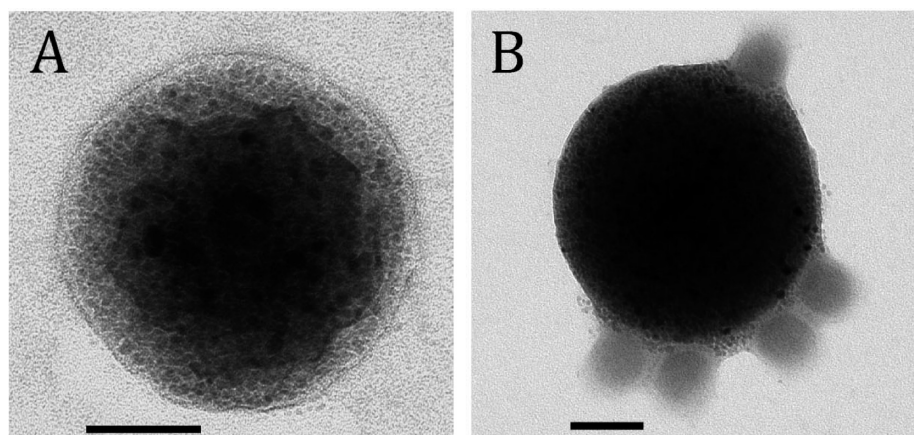


**Figure 1.** Transmission electron micrograph of a magnetic particle (left) and a MNP–Ad affinity complex (right). The samples were observed without staining using FEI Tecnai G2 electron microscope, Netherlands (bar = 100 nm). Note the large number of magnetite nanocrystals incorporated in the polymeric matrix of the particle and the multivalent character of the MNP–Ad association in A and B, respectively.

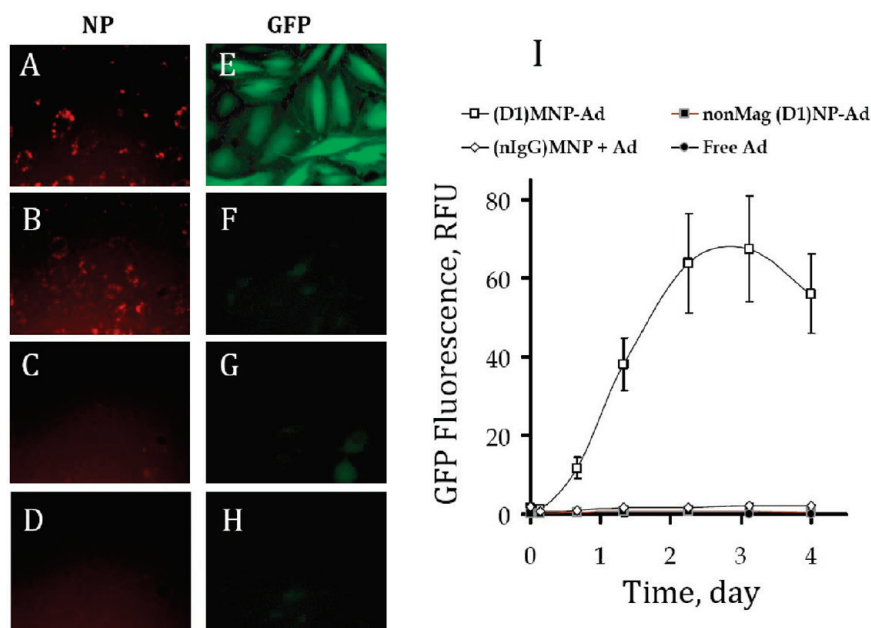


**Figure 2.** Intracellular localization of fluorescent-labeled nanoparticles (first column) and GFP expression (second column) in confluent A10 cells treated under magnetic conditions either with formulations combining  $GFP_{Ad}$  with D1-coated MNP (A, E), nIgG-coated MNP (B, F), analogous nonmagnetic NP (C, G), or with  $GFP_{Ad}$  alone (D, H). The cells were incubated with the formulations containing  $1.5 \times 10^7$  viral particles/well for 15 min in the presence of a nonuniform magnetic field (see Experimental Section), and the GFP expression and NP-associated fluorescence were observed 3 days post-treatment (the original magnification was  $\times 200$ ). GFP expression was quantified fluorimetrically ( $\lambda_{em}/\lambda_{ex} = 485 \text{ nm}/535 \text{ nm}$ ) over time (I).

Figure 2 shows the effect of the nanoparticle design on the transduction capacity of Ad affinity complexes under magnetic conditions. While a significant intracellular localization of MNP modified with either D1 or nIgG was exhibited after a 15 min magnetic exposure (Figure 2A,B), only D1-coated MNP could potentiate the gene transfer in cultured A10 cells (Figure 2E vs 2F). These results confirmed the requirement for the affinity MNP–Ad linkage in order to achieve more rapid cell binding and processing kinetics of the viral vector. Importantly, the gene transfer mediated by affinity complexes formed with D1-coated nonmagnetic particles was substantially less efficient than that of MNP–Ad

(Figure 2G vs 2E) in accordance with the insignificant cell association of the former after the 15 min incubation period (Figure 2C). The transduction enhancement specific to magnetically responsive complexes as opposed to Ad combined with either nonmagnetic particles or MNP modified with nIgG is shown quantitatively as a function of time

- (17) Polyak, B.; Fishbein, I.; Chorny, M.; Alferiev, I.; Williams, D.; Yellen, B.; Friedman, G.; Levy, R. J. High field magnetic gradients can target magnetic nanoparticle-loaded endothelial cells to the surfaces of steel stents. *Proc. Natl. Acad. Sci. U.S.A.* **2008**, *105*, 698–703.

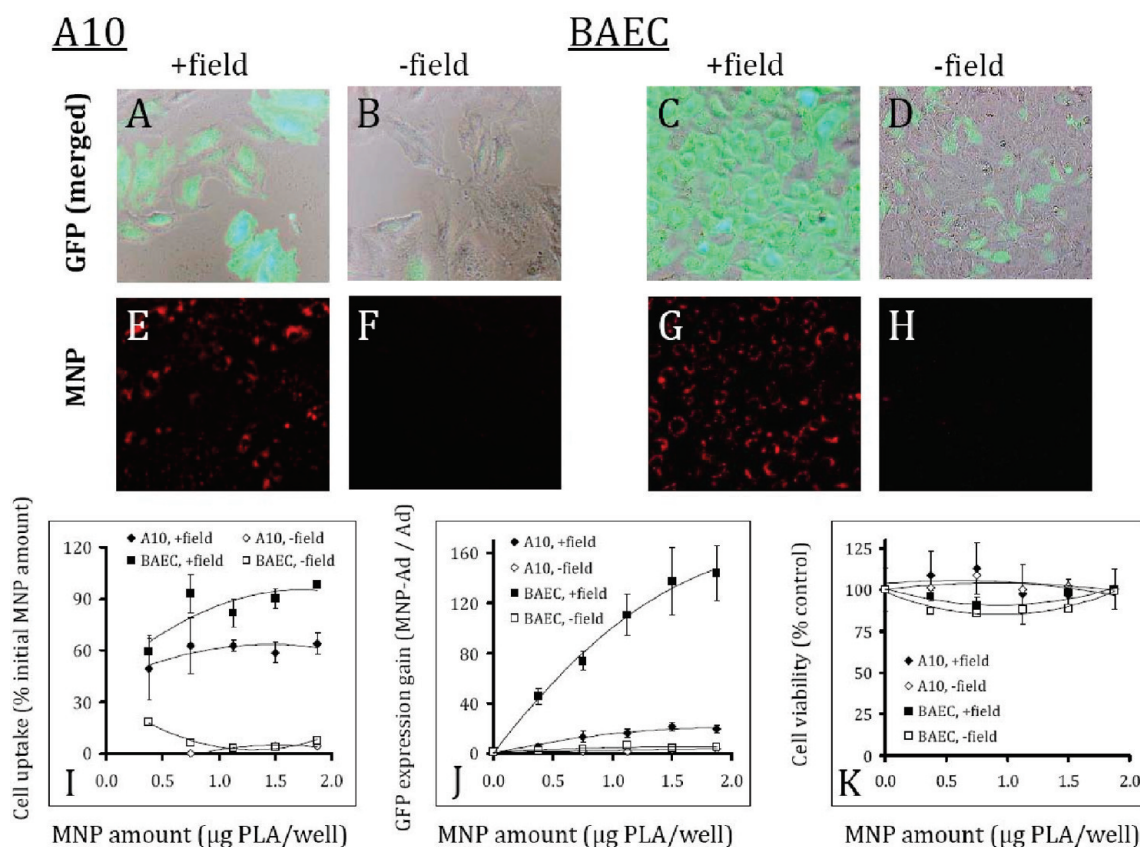


**Figure 3.** GFP expression (first row) and cellular localization of complex-forming MNP (second row) in A10 and BAEC observed microscopically 3 days after treatment under magnetic vs nonmagnetic control conditions (columns titled: “+ field” and “– field”, respectively). Merged GFP and bright field images of A10 (A, B) and BAEC (C, D) correspond to the red fluorescent micrographs showing cell-associated MNP (E, F and G, H for A10 and BAEC, respectively). The cells were seeded at a density of  $2 \times 10^3$ /well on day –1, and treated with MNP–Ad complexes formed using varying amounts of MNP and  $7 \times 10^7$  Ad/well on day 0. MNP uptake was determined by measuring the MNP-associated fluorescent signal ( $\lambda_{em}/\lambda_{ex} = 540 \text{ nm}/575 \text{ nm}$ ) and expressed as a fraction of the initially applied MNP that remained stably associated with the cells (I). Transduction efficiency was determined fluorimetrically ( $\lambda_{em}/\lambda_{ex} = 485 \text{ nm}/535 \text{ nm}$ ) 3 days post-treatment and presented as a fold increase in GFP expression vs free Ad for the sake of convenient comparison (J). The cell viability was determined by the Alamar Blue assay 3 days post-treatment using untreated cells as a control (K). The higher cell density of BAEC in comparison with A10 on the merged micrographs (3 days post-treatment) reflects the difference in the respective rates of cell growth under the employed experimental conditions. The original magnification was  $\times 200$ .

after cell treatment in Figure 2I. The maximal expression of GFP was observed in confluent A10 cells 3 days post-transduction followed by a decrease in the GFP fluorescent signal.

The observation of the magnetically enhanced gene transfer by Ad complexed with MNP was extended to dividing smooth muscle and endothelial cells in the experiment shown in Figure 3. A brief exposure to a high gradient magnetic field (average field gradient of 32.5 T/m) significantly increased the MNP–Ad mediated transduction in the both cell types compared to the respective “no field” controls (Figure 3A vs 3B and 3C vs 3D) in accordance with the more efficient cellular uptake under magnetic conditions (Figure 3E vs 3F and 3G vs 3H). This effect is shown quantitatively for MNP–Ad complexes formed using a range of MNP formulation amounts and a fixed Ad dose of  $7 \times 10^7$  per well (Figure 3I,J). Importantly, both the fractional MNP uptake and the gain in transduction presented as the

ratio of GFP expression mediated by MNP–Ad vs free Ad were directly dependent on the MNP formulation amount under magnetic conditions. The transduction gain increased from 45- to 144-fold, and from 5- to 20-fold for BAEC and A10 cells between the MNP doses of 0.4 and 1.9  $\mu\text{g PLA/well}$ , respectively (Figure 3J). At the same time, the viability of both cell types was not significantly affected in the studied MNP–Ad dose range following their treatment either with or without the presence of magnetic field (Figure 3K) remaining above 80% of that of the respective untreated cells.

The enhancing effect of the magnetic exposure on the MNP–Ad mediated gene transfer shown in Figure 3 for a range of MNP concentrations and the highest applied Ad dose was further confirmed with MNP–Ad formed using varying amounts of both formulation components (Figure 4A vs 4B and 4C vs 4D). The specific contribution of each variable under magnetic conditions was elucidated by

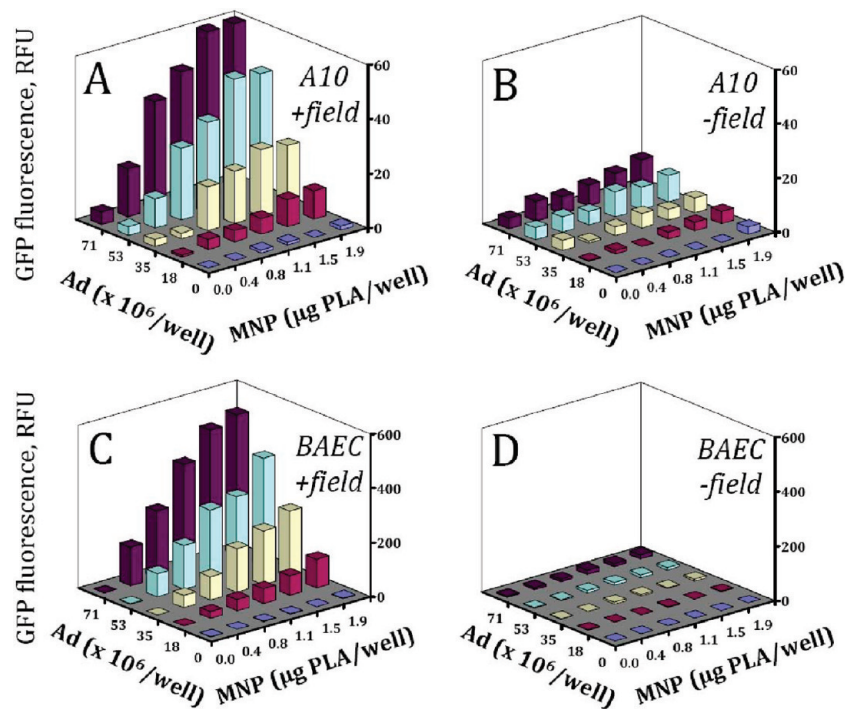


**Figure 4.** GFP expression mediated by MNP–Ad in A10 (top row) and BAEC (bottom row) under magnetic vs nonmagnetic conditions (left and right columns, respectively) as a function of MNP and Ad formulation amounts. GFP expression was measured fluorimetrically ( $\lambda_{em}/\lambda_{ex}$  = 485 nm/535 nm) in live cells 3 days post-treatment. Each data point represents an average of three experimental replicates.

**Table 1.** Regression Analysis of GFP Expression 3 Days Post-Transduction as a Function of the MNP and Ad Formulation Amounts Using the Second Order Model (Eq 1)<sup>a</sup>

model estimates	coeff estimates	<i>a</i>	MNP <sup><i>b</i></sup>	Ad <sup><i>c</i></sup>	MNP × MNP <sup><i>d</i></sup>	Ad × Ad <sup><i>e</i></sup>	MNP × Ad <sup><i>f</i></sup>
cell type: A10	coeff	0.46	5.32	−0.25	−4.06	0.00	0.53
Adj <i>R</i> <sup>2</sup> = 0.969	std error	2.38	4.01	0.10	1.91	0.00	0.04
<i>F</i> = 182	<i>t</i>	0.19	1.33	−2.46	−2.13	3.86	12.59
<i>p</i> < 0.001	<i>p</i>	0.849	0.197	0.021	0.044	<0.001	<0.001
cell type: BAEC	coeff	1.67	19.94	−1.36	−15.52	0.02	4.10
Adj <i>R</i> <sup>2</sup> = 0.987	std error	11.70	19.71	0.50	9.38	0.01	0.21
<i>F</i> = 427	<i>t</i>	0.14	1.01	−2.697	−1.65	3.88	19.94
<i>p</i> < 0.001	<i>p</i>	0.888	0.322	0.013	0.111	<0.001	<0.001

<sup>a</sup> Adjusted *R*<sup>2</sup> (Adj *R*<sup>2</sup>) gives the ratio of variance explained by the model to total variance in the measured data and assumes values between 0 and 1. Similarly, the *F* statistic provides the ratio of variance explained by the model to unexplained variance and can take values  $\geq 1$ . Together with the *p* statistic, the Adj *R*<sup>2</sup> and *F* are measures of the model adequacy (see model estimates). The *t* statistic in the coefficient estimates is the ratio of a select regression coefficient to its standard error, and determines the contribution of an individual term in the model to the experimental data. Its absolute value may be equal to zero (no contribution to the experimental data) or higher.

multiple regression analysis using the GFP expression measurements in A10 cells and BAEC three days post-treatment presented in Figure 4A and 4C, respectively. The initial results showed that the data were not described satisfactorily by a simple first order model considering only the linear effects of the variables. However most of the variance in the GFP expression was accounted for by corresponding second order models that consider both the linear and quadratic effects of the individual variables and their interactions (adjusted *R*<sup>2</sup> of 0.97 and 0.99 for A10 and BAEC, respectively):

$$\text{GFP} = a + b \times \text{MNP} + c \times \text{Ad} + d \times \text{MNP}^2 + e \times \text{Ad}^2 + f \times \text{MNP} \times \text{Ad} \quad (1)$$

where *a* is the constant term, *b–f* are the regression coefficients, GFP is the measured GFP fluorescence, MNP is the formulation amount of the particles, and Ad is the formulation amount of the virus.

The results of the regression analysis are summarized in Table 1. The second order model was found to be valid for the both types of cells and provided an indication of a strong dependence of the transgene expression on the selected variables (*F* statistic equaling 182 and 427 for A10 and BAEC, respectively). Importantly, the terms related to the linear and quadratic effects of the MNP formulation amount on the transduction efficiency were either borderline significant or nonsignificant, and did not contribute substantially to the observed GFP expression as suggested by their



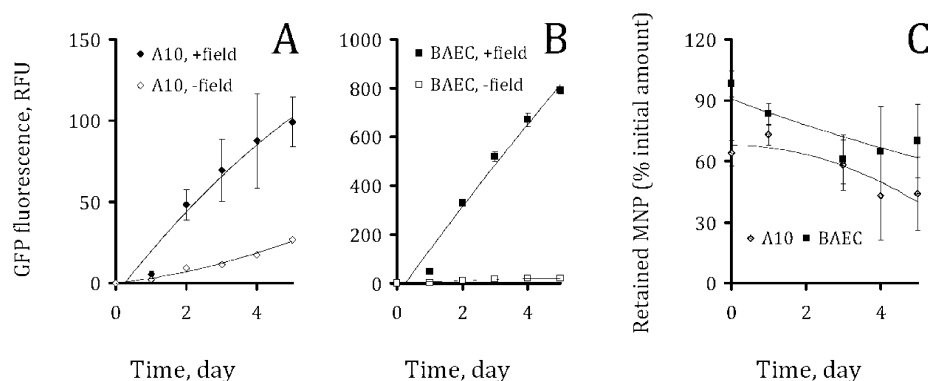


**Figure 5.** The kinetics of GFP expression by A10 cells (A) and BAEC (B) treated with magnetic affinity complexes formed at MNP and Ad formulation amounts of  $1.9 \mu\text{g}$  PLA and  $7.1 \times 10^7$  per well, respectively. The kinetics of MNP elimination was expressed as the fraction of the initially applied MNP retained by the cells by a given time point (C).

respective  $t$  values. While the individual effects of Ad, both linear and quadratic, were statistically significant for both cell types, their contribution to the overall transduction became evident only at the highest Ad doses accounting for 5–10% of the total variance in GFP expression. The most pronounced effect as indicated by the corresponding  $t$  and  $p$  values was associated with the interaction between MNP and Ad described by the MNP  $\times$  Ad term of the model equation, demonstrating that the majority of the gene transfer in both A10 and BAEC was mediated by the affinity complexes rather than Ad alone under magnetic conditions.

The kinetics of the transgene expression and elimination of the fluorescent MNP–Ad complexes was studied in dividing cells over a 5 day period. The expression profiles shown for the cells treated with the complexes formulated using the highest doses of MNP and Ad (Figure 4A and 4B for A10 and BAEC, respectively) are representative of the pattern observed with MNP–Ad formed at other examined MNP to Ad ratios (data not shown for the sake of simplicity). Endothelial cells exhibited substantially higher transduction rates at equivalent MNP–Ad doses in comparison to A10 (Figure 5A,B). Notably, the GFP expression by the cells of the both types increased over a 5 day period in contrast with the bell-shaped kinetic pattern characteristic of the contact-inhibited cells (Figure 2I), reflecting a progressively growing number of cells contributing to the total green fluorescent signal in the former case. Interestingly, the elimination of the particles as estimated from the change in the cell-associated red fluorescence occurred at a relatively slow rate with a decrease of  $\sim 30\%$  over a 5 day period observed in the both cell types (Figure 5C).

## Discussion

The use of biocompatible MNP as a platform for Ad-mediated gene delivery represents a novel approach addressing a number of limitations inherent to this gene delivery vector. Vector-specific affinity complexation of Ad with biodegradable polymeric NP was previously proposed by our group as a means to achieve facilitated CAR-independent cellular uptake and enhanced transgene expression in cells otherwise nonpermissive to adenoviral transduction.<sup>11</sup> In this

study we investigated a modification of this strategy utilizing superparamagnetic complex-forming NP that endow the formulation with magnetic responsiveness. In the clinical setting the kinetically favorable CAR-detargeted vector processing combined with magnetically enhanced delivery demonstrated in the present *in vitro* studies may translate into lower vector doses required for achieving a therapeutically adequate effect and, as a result, a reduction in the systemic untoward reactions associated with Ad.

The MNP complexation strategy relies on preformed carrier particles whose magnetic properties, size, surface chemistry, biodegradation rate and colloidal stability can be controlled by adjusting the formulation conditions.<sup>13</sup> Importantly, the binding of the virus to the particles does not require its chemical modification and/or exposure to the harsh conditions employed in most polymeric NP preparation methods. Thus the functionality of the vector remains uncompromised, while its association with the MNP surface via a dissociable affinity bond ensures its ready availability that is typically reduced in the experimental approaches attempting Ad entrapment in the polymeric particle core.<sup>18,19</sup> It is of note that the same MNP preparation can be used to form complexes with different types of Ad vectors or different MNP/Ad stoichiometries, thus facilitating a comparison between different complex compositions and transgenes<sup>11</sup> and simplifying formulation optimization. The applicability of this approach can potentially be extended to include viral vectors other than Ad by selecting an appropriate affinity adaptor molecule for the MNP surface modification.<sup>20</sup>

- (18) Mok, H.; Park, J. W.; Park, T. G. Microencapsulation of PEGylated adenovirus within PLGA microspheres for enhanced stability and gene transfection efficiency. *Pharm. Res.* **2007**, *24*, 2263–9.
- (19) Turner, P.; Petch, A.; Al-Rubeai, M. Encapsulation of viral vectors for gene therapy applications. *Biotechnol. Prog.* **2007**, *23*, 423–9.
- (20) Mah, C.; Fraites, T. J., Jr.; Zolotukhin, I.; Song, S.; Flotte, T. R.; Dobson, J.; Batich, C.; Byrne, B. J. Improved method of recombinant AAV2 delivery for systemic targeted gene therapy. *Mol. Ther.* **2002**, *6*, 106–12.

In this study a substantial enhancement of Ad-mediated gene transfer was demonstrated with D1-modified MNP under magnetic conditions, whereas little to no increase in transduction was observed with any of the control treatments. Such specificity of the transduction enhancing effect confirms the requirement for a strong yet reversible vector–carrier association and an adequate magnetic susceptibility of the formulation. The latter is essential for providing an efficient localization and protracted presence of the vector at the injury site when used in the context of in-stent restenosis treatment. The site-specific delivery in this setting can be accomplished with a novel concept of vector targeting to magnetizable implants, such as stainless steel stents, in the presence of a strong uniform field.<sup>21</sup> The feasibility of this strategy has been proven in a number of recent studies by our group.<sup>17,22</sup>

The rates of magnetically governed transduction by MNP–Ad complexes correlated with the internalization of the complex-forming D1MNP and exhibited a direct dependence on the Ad and MNP formulation amounts in the both studied vascular cell types. To elucidate the specific role of the two variables on the transduction capacity of the complexes, the transgene expression was analyzed by multiple regression. This methodology has been well-established for the optimization of formulation parameters.<sup>23–25</sup> To our knowledge the present study is the first example of its use for evaluating the performance of particle–virus hybrid systems. Notably, a transduction mechanism distinct from that of free Ad was suggested by the GFP expression pattern of MNP–Ad treated cells. The significant interaction between the two formulation variables confirms that the transduction enhancement under magnetic conditions is MNP-dependent and thus is associated with the MNP–Ad complexes. The contribution of free Ad to the total GFP fluorescence in the two cell types becomes significant only at the highest examined stoichiometrical ratios of Ad to MNP, indicating that the binding capacity of the MNP may

be exceeded under these conditions. The optimal range of the respective MNP and Ad amounts may thus be defined where the fraction of the unbound Ad is minimized, and the vector is efficiently magnetically localized and retained at the stented arterial segment. This is also essential for reducing the Ad concentration-dependent adverse reactions associated with the virus escape to nontarget tissues.

Importantly, the magnetically enhanced transduction achieved the high levels of gene transfer in cultured cells after a brief exposure of 15 min and with the Ad dose in the range significantly lower than previously applied with nonmagnetic NP–Ad affinity complexes.<sup>11</sup> While the elimination of the internalized complexes was shown to be a relatively slow process, the viability and the growth kinetics of the transduced cells remained unaffected by the treatment (Figures 3 and 5) providing evidence for biocompatibility of the magnetic formulation.

The size of the affinity complexes (400–420 nm), while a potential limitation of their use for systemic administration that is likely to result in rapid sequestration by the reticuloendothelial system,<sup>26</sup> makes them well-suited for local delivery to magnetizable implants as proposed by our group.<sup>21,22</sup> The high magnetic susceptibility of the carriers in this size range is expected to increase both their magnetic capture and retention in the targeted region.<sup>21</sup> In addition to the previously shown utility of MNP–Ad complexes for site-specific gene delivery to stented arteries,<sup>22</sup> MNP–Ad mediated transduction can be used as a part of a targeted cell therapy strategy.<sup>17</sup> In the context of this treatment scheme MNP–Ad could be applied for *ex vivo* modification of autologous cells to achieve both magnetic cell loading and expression of a therapeutic transgene. Targeting to a magnetizable stent in the presence of a uniform magnetic field can then be employed for delivery of genetically modified cells to the injured vessel.<sup>17</sup>

In conclusion, the enhancement of Ad-mediated gene delivery by affinity complexation with biodegradable MNP represents a novel and interesting method for improving and extending the applicability of the viral gene therapeutic strategies. Additional studies employing novel magnetic targeting delivery concepts need to be designed for conclusive evaluation of the *in vivo* therapeutic potential of this approach.

**Acknowledgment.** The authors acknowledge the assistance of Ms. Susan Kerns in the preparation of this manuscript. This research was supported in part by grants from the American Heart Association (M.C., I.F.), The National Institutes of Health, HL72108 (R.J.L.), and the William J. Rashkind Endowment of The Children's Hospital of Philadelphia.

MP900017M

- (21) Yellen, B. B.; Forbes, Z. G.; Halverson, D. S.; Fridman, G.; Barbee, K. A.; Chorny, M.; Levy, R.; Friedman, G. Targeted drug delivery to magnetic implants for therapeutic applications. *J. Magn. Magn. Mater.* **2005**, 293, 647–54.
- (22) Yellen, B. B.; Chorny, M.; Fishbein, I.; Dai, N.; Ottey, A.; Klingerman, C.; Alferiev, I.; Nyanguile, O.; Friedman, G.; Levy, R. J. Site specific gene delivery using magnetic forces to localize adenoviral vector-magnetic nanoparticle complexes to stented arterial segments. *Circulation* **2005**, 112 17 (Suppl. II), 653.
- (23) Molpeceres, J.; Guzman, M.; Aberturas, M. R.; Chacón, M.; Berges, L. Application of central composite designs to the preparation of polycaprolactone nanoparticles by solvent displacement. *J. Pharm. Sci.* **1996**, 85, 206–13.
- (24) Wehrle, P.; Magenheimer, B.; Benita, S. The influence of process parameters on the PLA nanoparticle size distribution, evaluated by means of factorial design. *Eur. J. Pharm. Biopharm.* **1995**, 41, 19–26.
- (25) Attivi, D.; Wehrle, P.; Ubrich, N.; Damge, C.; Hoffman, M.; Maincent, P. Formulation of insulin-loaded polymeric nanoparticles using response surface methodology. *Drug Dev. Ind. Pharm.* **2005**, 31, 179–89.

- (26) Moghimi, S. M.; Hunter, A. C.; Murray, J. C. Long-circulating and target-specific nanoparticles: theory to practice. *Pharmacol. Rev.* **2001**, 53, 283–318.